PROCEEDINGS, 49th Workshop on Geothermal Reservoir Engineering
Stanford University, Stanford, California, February 12-14, 2024
SGP-TR-227

Study on the effect of basalt fiber, styrene butadiene latex, and epoxy resin on geothermal cement performance

You Ye[a], Huijing Tan[a,*], Yao Chen[a], Xiyue Cui[a]

[a] College of Environment and Civil Engineering, Chengdu University of Technology, Chengdu, 610059, China

yeyou@stu.cdut.edu.cn

Keywords: Basalt fiber; styrene butadiene latex; mechanical properties; class G oil well cement; epoxy resin.

ABSTRACT

To address the issues of cement ring brittleness failure and gas channeling in geothermal and oil and gas cementing, it is often necessary to incorporate fiber, latex, resin and other toughening materials into the cement. This study aims to investigate the effect of basalt fiber (BF), styrene butadiene latex (SBL), and epoxy resin (ER) on the performance of class G oil well cement. Different proportions of BF, SBL and ER were added into the cement slurry, and their rheological properties, setting time, and mechanical properties were tested. The microstructure of the mixture with good performance was further examined. The test results indicate that good rheological and mechanical properties could be obtained by the cement with 0.6% BF and 10% SBL. The 7 days compressive and flexural strength of the optimized cement formula are 28.6 MPa and 3.7 MPa, respectively. The development of cement microcracks can be controlled by BF through bridging and friction. The addition of SBL makes the cement matrix become denser and improves the strength and toughness of cement with BF.

1. INTRODUCTION

In the oil and gas and geothermal development process, complex environments such as high temperature, high pressure, and corrosion, as well as construction operations like perforation, fracturing, and well completion, can cause brittle failure of cement, resulting in micro-cracks and leading to issues like oil well gas migration, annular pressure, and corrosion gas leakage in oil wells. These problems can severely affect the cementing quality and reduce their production life (Liu et al 2014; Zhou et al 2009; Zhou et al 2008; Li et al 2004). Therefore, it is necessary to add additives to the cement slurry to improve the toughness and long-term sealing ability of the cement (Li et al 2016; Li et al 2008; Hua and Yao 2007).

Cementing cement toughening systems mainly include fiber cement slurry systems, latex cement slurry systems and elastic particle cement slurry systems. Traditional fiber-cement matrix composites have high toughness but poor dispersion and do not bind tightly with cement. Basalt fiber (BF), a new type of inorganic mineral fiber, has high elastic modulus, wear resistance, strong tensile properties, good compatibility with cement, easy availability, and is environmentally friendly (Li et al 2022; Monaldo et al 2019; Dhand et al 2014). Therefore, BF has great potential for toughening oil well cement. Heng et al (2016) found that after adding 0.2% BF to cement, the formation and development of micro-cracks in cement were controlled, and the fiber bonded tightly with the hydration products of cement. Luo et al (2015) found that when the BF content was 0.5%, the tensile strength of the cement could be increased by 50%, and the elastic modulus of cement could be reduced, improving its toughness. Gao et al (2018) found that adding BF could improve the compressive strength of concrete, with better results when the fiber length was 6 mm. The crack resistance of the fiber increased the overall compressive strength of concrete.

However, the "agglomeration" phenomenon of single fiber and the weak layer between the fiber and the cement interface are not conducive to improving the compressive strength of the cement, so it is necessary to consider adding multiple toughening materials to work together in the cement paste. Qi et al (2016) developed butadiene-styrene latex (SBL) BZT-L1, which showed good fluidity when added to the slurry. The 24 h compressive strength of the cement slurry was greater than 14 MPa. Yan et al (2017) found that by adding epoxy resin (ER) to cement, the compressive strength of the cement increased with the increase of epoxy resin content. Liu et al (2019) added 60% ER to the cement, and the 28 days compressive strength, tensile strength, and elastic modulus of cement were 51 MPa, 5.1 MPa, and 1.8 GPa, respectively. Wu et al (2019) found that when 0.2% carbon fiber and 1% latex were mixed, the compressive strength, flexural strength and impact strength of cement were 35.44 MPa, 11.15 MPa and 2.08 kJ/m^2, respectively, and the elastic modulus reached 5.8 GPa. Li et al (2020) mixed an appropriate amount of polypropylene fiber with latex and found that the fiber mixture could to some extent solve the problem of reduced strength of latex cement and enhance the stability of the cement slurry.

At present, there are many studies on single-component toughening cement slurry systems, but there are fewer studies on multi-component composite cement slurry systems, especially BF multi-component composite cement slurry systems. Therefore, this paper investigates the mechanical properties of G-grade oil well cement, single-doped BF cement, BF-SBL cement, and BF-ER (without curing agent) cement. FTIR, SEM, XRD and MIP tests were also conducted on the best formula to characterize its performance.

2. EXPERIMENTAL DETAILS

2.1 Materials

In the experiment, G-class oil well cement produced by Sichuan Jiahua Special Cement Co., Ltd. was used. BF (12 mm in length, density of 2.63 g/cm^3) was produced by Changzhou Tianyi Engineering Fiber Co., Ltd., and SBL was provided by Jinan Luchu Rubber Chemical Co., Ltd. ER (E-44), stabilizer tween 60 (polyoxyethylene sorbitan monostearate), and defoamer were provided by Shandong Yousuo Company.

2.2 Sample Preparing

In the experiment, different proportions of additives were added to the cement slurry. The experimental formulas are shown in Table 1, where S, E and B represent SBL, ER and BF, respectively, and the numbers represent the amounts added. For example, S5E0B0.3 means the amounts of SBL and BF added are 5% and 0.3%, respectively, and W/C represents the water-cement ratio. After the cement slurry was mixed, the density, fluidity, and setting time of cement slurry were tested. The prepared slurry was poured into rectangular mods of 50 mm ×50 mm ×150 mm and cylindrical molds H:150 mm R: 25 mm for flexural strength and compressive strength tests, respectively. After curing at 20 ℃ for 24 h, the samples were demolded and placed under constant temperature and pressure conditions of 20℃ and 0.1 MPa to cure for 7 days.

Table 1: Experimental recipes.

NO	cement (g)	SBL(%)	ER(%)	BF(%)	Stabilizer(%)	Defoamers(%)	W/C
S0E0B0	100	0	0	0	0.3	0.3	0.44
S0E0B0.3	100	0	0	0.3	0.3	0.3	0.44
S0E0B0.6	100	0	0	0.6	0.3	0.3	0.44
S5E0B0.3	100	5	0	0.3	0.3	0.3	0.44
S5E0B0.6	100	5	0	0.6	0.3	0.3	0.44
S10E0B0.3	100	10	0	0.3	0.3	0.3	0.44
S10E0B0.6	100	10	0	0.6	0.3	0.3	0.44
S0E3B0.3	100	0	3	0.3	0.3	0.3	0.44
S0E3B0.6	100	0	3	0.6	0.3	0.3	0.44
S0E6B0.3	100	0	6	0.3	0.3	0.3	0.44
S0E6B0.6	100	0	6	0.6	0.3	0.3	0.44

2.3 Mechanical property testing

The compressive strength of cement slurries was tested by WHY-1000 computer-controlled pressure testing machine (Shanghai Hualong Testing Instrument Co., Ltd.). The flexural strength was tested by YAW-300 D automatic cement flexural and compressive testing machine. Each test group contained 3 specimens and the average strength of 3 test specimens was calculated as the final strength.

2.4 X-ray diffraction (XRD)

To identify the hydration products of cement stone after adding additives, XRD (Bruker D8 advance) was used to test the samples. Before testing, specimens were soaked in anhydrous ethanol for 24 hours to prevent further hydration and then dried in an oven for 24 hours.

2.5 Fourier transform infrared (FTIR)

The remaining samples after the mechanical tests were also ground into a uniform powder for infrared spectroscopy tests. In this paper, Fourier transform infrared spectrometer (Thermo Scientific Nicolet iS5) was used to characterize the chemical bonds of cement stone hydration products.

2.6 Scanning Electron Microscope (SEM)

After the mechanical tests, the remaining samples were made into 1 cm× 1 cm thin section for SEM to observe the interfacial bonding between cement stone and additives. The samples were gold-sputtered before SEM testing.

2.7 Mercury intrusion porosimetry (MIP)

The effect of additives on the porosity and pore size distribution of the samples was analyzed by mercury intrusion porosimetry (AutoPore9500).

3. RESULTS AND DISCUSSION

3.1 Workability

3.1.1 Fluidity

The fluidity data of all specimens are shown in table 2. The fluidity of the pure cement slurry S0E0B0 is 141 mm. However, it can be observed that the addition of admixtures significantly changes the fluidity of the cement slurry. The fluidity of the S0E0B0.6 cement slurry is the lowest, with a fluidity of 101 mm. This is due to the BF absorbing, reducing the free water content of cement slurry (Zhu et

al 2022). The highest fluidity of the S10E0B0.3 cement slurry is 237 mm, which is caused by the increase of free fluid in the cement slurry after the addition of SBL (Wang et al 2006). However, with the same amount of SBL added, the fluidity of the S10E0B0.6 cement slurry is 213 mm, indicating that the fluidity of the cement slurry decreases with the increase of BF. After mixing ER with BF, the fluidity of S0E3B0.6, S0E6B0.3 and S0E6B0.6 are 118 mm, 125 mm and 112 mm, respectively. The above data indicates that the fluidity of single-doped BF cement slurry and BF-ER cement slurry cannot meet the construction requirements of 140 mm.

Table 1: Working performance of cement slurry.

NO	Fluidity (mm)	Density(%)	Initial setting time(h)	Final setting time (h)
S0E0B0	147	1.92	6	7.5
S0E0B0.3	103	1.98	5	6
S0E0B0.6	101	1.94	4.5	5.5
S5E0B0.3	177	1.94	7	8.5
S5E0B0.6	175	1.91	6	7.5
S10E0B0.3	237	1.96	8	9.5
S10E0B0.6	213	1.97	7.5	8.75
S0E3B0.3	145	1.93	6.5	7.5
S0E3B0.6	118	1.9	6.75	8
S0E6B0.3	125	1.94	7	8
S0E6B0.6	112	1.88	7.25	8

3.1.2 Density

As shown in table 2, the effect of admixture content on the density of cement slurry is minimal. Notably, after adding 0.3% BF, the density of the cement increases slightly. When the content of BF is 0.6%, the density of cement slurry decreases, which is due to the formation of more voids by a large number of fibers in the cement slurry.

3.1.3 Setting time

Table 2 presents the initial and final setting time of cement. It can be seen that the initial setting time of pure cement slurry is 6 hours, and the final setting time is 7.5 hours. However, compared to pure cement slurry, the setting time of BF cement slurry shortens. Among them, setting time of S0E0B0.6 cement slurry is the shortest, with an initial setting time of 4.5 hours and a final setting time of 5.5 hours. This phenomenon indicates that adding BF to the cement slurry can advance the setting time of the cement slurry. Compared to pure cement slurry, the setting time of cement slurry extends after adding SBL, and the initial and final setting time of cement slurry increase with the increase of SBL. The initial and final setting time of S10E0B0.3 cement slurry reach the longest at 8 hours and 9.5 hours, respectively (Lu et al 2016; Ray et al 1995; Kong et al 2015). Compared to pure cement slurry, the setting time of BF-ER cement slurry increases slightly, indicating that ER can delay the solidification of the cement slurry.

3.2 Mechanical properties

3.2.1 Compressive Strength

Figure 1 shows the 7 days compressive strength of samples with different admixtures. As shown in Figure 1, the compressive strength of the samples decreases after the addition of admixtures (Shafieyzadeh 2013; Ukrainczyk and Rogina 2013). The highest compressive strength of pure cement paste is 38.9 MPa at 7 days. Compared to pure cement paste, the compressive strength of single-doped BF cement paste decreases by about 60%, which may be due to the use of BF in a bundled form, occupying a large space (Jiang et al 2014; Chen et al 2013). At the same time, the water absorption of the fibers reduces the free liquid content in the cement slurry, resulting in insufficient hydration reaction and a decrease in compressive strength of the cement paste. Notably, the 7 days compressive strength of S0E6B0.6 cement paste is 10.7 MP, 72.5% lower than that of pure cement paste, indicating that the mixture of low-content ER and BF exacerbates the reduction in compressive strength of cement paste (Song et al 2022; Jin et al 2022). Compared to pure cement paste, the compressive strength of S10E0B0.6 cement paste decreases by 26.5%, with a compressive strength of 28.6 MPa. However, the compressive strength of SBL-BF cement paste is 82.2% higher than that of single-doped BF cement paste. This demonstrates that the addition of SBL can improve the compressive strength of BF cement paste. The reason is that SBL can enter the weak layer between the fiber-cement interface, making the cement paste denser and improving the compressive strength of the cement paste.

3.2.2 Flexural strength

The 7 days flexural strength of cement paste is shown in Figure 2. The flexural strength of cement paste with admixture decreases compared to that of pure cement paste, which is consistent with the compressive strength situation. The flexural strength of S0E0B0

cement paste is 5.9 MPa. The flexural strength of S0E0B0.3 and S0E0B0.6 cement paste are 3.5 MPa and 3.9 MPa, respectively, and 40.1% and 33.9% lower than that of pure cement paste. The uneven distribution of BF in the cement paste may be the reason for the decrease in flexural strength. The flexural strength of S5E0B0.6 and S10E0B0.6 cement paste are 3.5 MPa and 3.7 MPa, respectively, indicating that, with a constant BF content (0.6%), the flexural strength of cement paste increases as the amount of SBL increases. The lowest flexural strength is 2.6 MPa for S0B3L0.3, a decrease of 55.9%, indicating that this combination of ER- BF is the most detrimental to the flexural strength of cement paste.

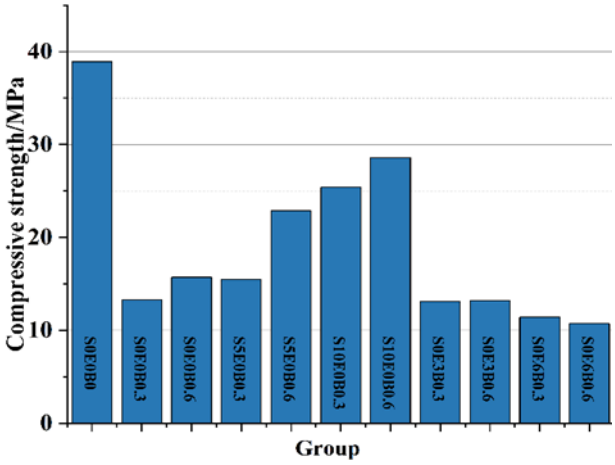

Figure 1: The 7 days compressive strength of each cement stone.

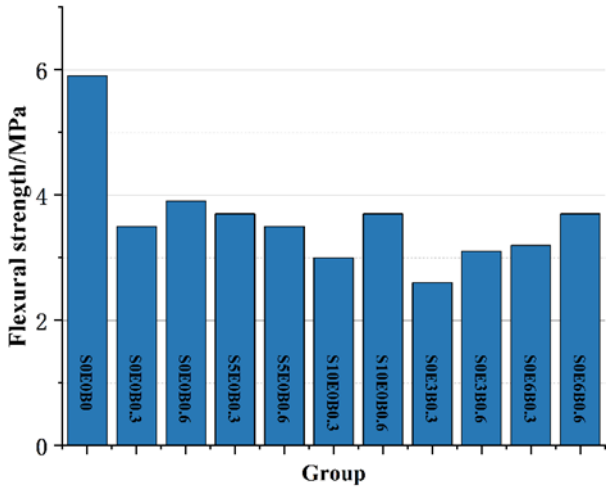

Figure 2: The 7 days flexural strength of each cement stone.

In summary, the comprehensive performance of cement paste mixed with ER and BF is not as good as that of single BF cement paste, while the comprehensive performance of cement paste mixed with SBL and BF is better. Although the compressive and flexural strength of BF-SBL cement paste are slightly lower than those of pure cement paste, they still meet the requirements for cementing construction. To further explore the mechanism of action of BF and SBL in cement paste, microscopic tests were conducted on BF-SBL cement paste with different contents.

3.3 Micro performance tests

3.3.1 XRD

The XRD patterns of BF-SBL cement paste is shown in Figure 3. From Figure 3, it can be observed that the shape of each diffraction peak is basically similar, indicating that the addition of different proportions of BF and SBL does not change the hydration products of oil well cement. The peak near 32° in 2 θ indicates that the intensity of C_3S and C_2S diffraction peaks increases with the increase of SBL, while the peak at 34° in 2 θ indicates that the intensity of $Ca(OH)_2$ diffraction peaks decreases with the increase of SBL. This demonstrates that SBL reduces the hydration of cement and inhibits the formation of $Ca(OH)_2$. Therefore, SBL can to some extent slow down the corrosion of cement stone by slowing down the reaction between corrosive gas and $Ca(OH)_2$.

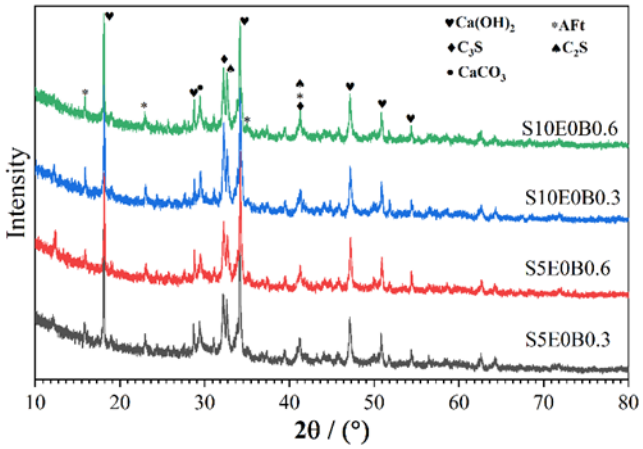

Figure 3: The XRD of BF-SBL cement stone.

3.3.2 FTIR

Figure 4 shows the FTIR of BF-SBL cement stone with different dosages. As can be seen from Figure 4, the most noticeable peak is at 3440 cm^{-1}, which corresponds to the N-H stretching vibration; 2924 cm^{-1} and 2855 cm^{-1} are the asymmetric and symmetric stretching vibration of C-H in C-CH-C; at 1643 cm^{-1}, there is the C=0 stretching vibration peak; 1412 cm^{-1} is the stretching vibration peak of aromatic benzene ring skeleton in SBL. The hydration products of cement stone are similar under different dosages of admixtures. The results indicate that different additives do not change the hydration products of cement.

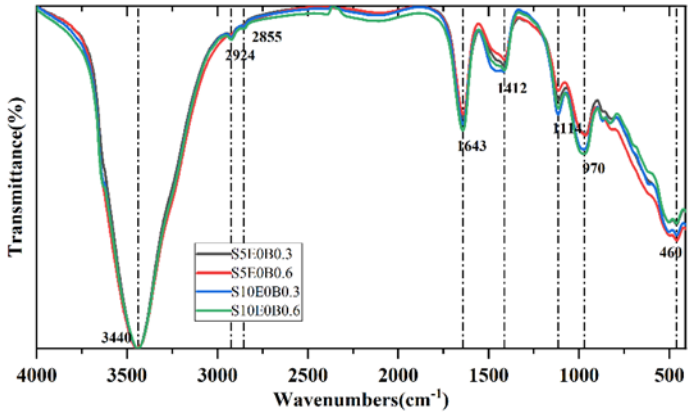

Figure 4: FTIR of BF-SBL cement stone.

3.3.3 SEM

Figure 5 (a, b, c) and (d, e, f) are SEM images of S5E0B0.3 and S5E0B0.6 cement paste respectively, while Figure 6 (a, b, c) and (d, e, f) are SEM images of S10E0B0.3 and S10E0B0.6 cement paste, respectively. After mixing BF with SBL, most of the BF in the cement stone appear in a bundle shape, as shown in Figure 5 (c, f) and 6 (c, f). From Figure 1 (a), it can be seen that a small amount of SBL is covered on the cement matrix. According to Figure 5(b) and 6(a), cement hydration products can be observed adhering to the fiber surface, indicating that BF have good compatibility with cement (Khandelwal and Rhee 2020). In Figure 6 (b), bonding tightness at the interface between BF and cement matrix is better than that in Figure 5 (b). The reason is that with the increase of SBL, the gaps at the fiber-cement interface are gradually filled by SBL. At the same time, by comparing the cement matrix in Figure 5 and Figure 6, it is found that the higher the amount of SBL, the denser the cement matrix, indicating that SBL can indeed refine the pore size of cement paste. It can be observed from Figure 5 (f) that when a large crack vertically passes through the BF, the crack width decreases sharply. The reason is that the fiber inhibits the development of cracks through "bridging" and friction, so the crack width decreases after passing through the fiber (Silva et al 2009; Reis 2006; Zhu et al 2022). If the fiber continues to be subjected to external forces, the fibers will be pulled out or broken, as shown in Figure 5 (b, e) and Figure 6 (b, c). It can be seen that the mixture of SBL and BF can make the cement stone matrix denser, fill the gaps between fiber and cement, limit the development of cement stone cracks, and improve the toughness of cement stone (Yang et al 2019).

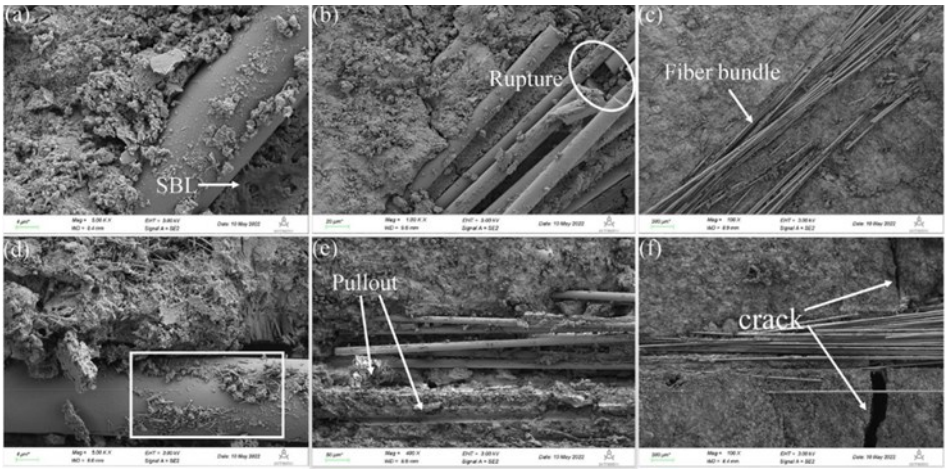

Figure 5: SEM of S5E0B0.3 and S5E0B0.6 cement stone.

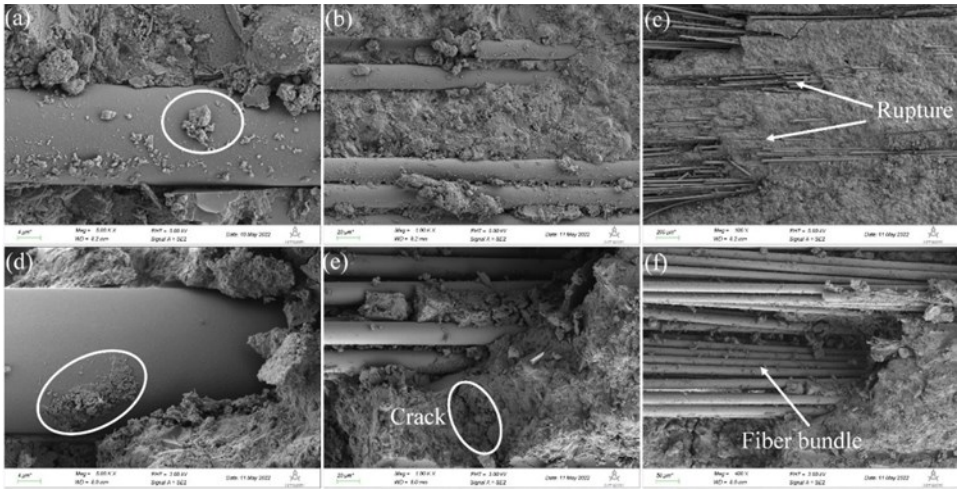

Figure 6: SEM of S10E0B0.3 and S10E0B0.6 cement stone.

3.3.4 MIP

Figure 7 describes the porosity of cement stone mixed with different BF and SBL. It can be found from Figure 7 that the cement stone with the lowest porosity is S10E0B0.3, at 20.37%, while the highest porosity is S5E0B0.6, at 24.03%. The porosity of S5E0B0.6 is 1.86% higher than that of S5E0B0.3, and the porosity of S10E0B0.6 is 0.66% higher than that of S10E0B0.3. This indicates that the porosity of cement paste increases with the increase of BF content, and the increase magnitude decreases with the increase of SBL content (Li et al 2020). Combined with SEM images, it can be observed that BF appear in bundles after being added to cement stone, occupying a large space and leading to an increase in porosity. The addition of SBL can fill the voids between fiber-cement matrix interface, refine the pore size of cement stone, and thus reduce their porosity (Karakosta et al 2015).

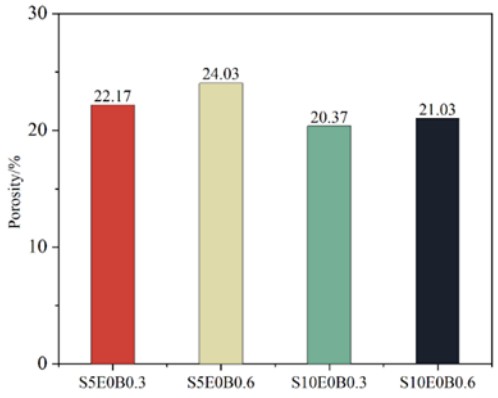

Figure 7: Porosity of BF-SBL cement stone.

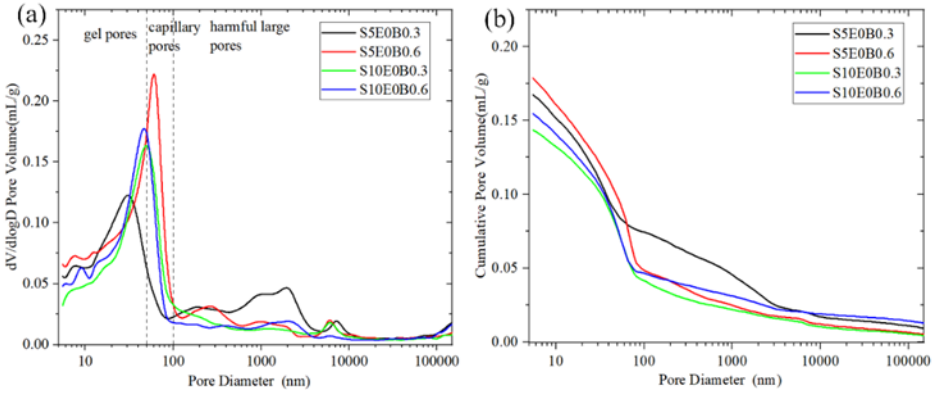

Figure 8: Accumulated pore volume of cement stone.

Table 3 shows the MIP data of BF-SBR cement stone with different dosages. It can be observed from Table 3 that the total pore volume of S10E0B0.3 is the lowest at 0.1433 ml/g, while the maximum pore volume of S5E0B0.6 is 0.1789 ml/g. Compared with S5E0B0.3, the total pore volume of S10E0B0.3 decreases with the increase of SBL content, with a reduction rate of 14.4%. Comparing with S5E0B0.6, the total pore volume of S10E0B0.6 decreases with the increase of SBL content, with a total pore volume reduction rate of 13.6%. This indicates that the addition of SBL can reduce the total pore volume of cement stone.

Table 3: Cement stone MIP data.

NO	V-total(ml/g)	Average pore size(4V/A)	Intermediate pore size V(nm)	Intermediate pore size A(nm)
S5E0B0.3	0.1675	31.3	53.5	12.6
S5E0B0.6	0.1789	29.2	56.8	12.7
S10E0B0.3	0.1433	32.1	52.7	15.5
S10E0B0.6	0.1545	30.3	49.8	13.9

The pore size distribution and cumulative pore size distribution of BF-SBL cement paste were plotted through MIP testing, as shown in Figure 8. By observing Figure 8(a), it can be found that the pore size of cement stone mixed with BF and SBL is mainly distributed in the range of 10-100 nm. The proportion of harmful large pores is the highest in S5E0B0.3 cement stone. The reason is that BF are in bundles, and bubbles generated during cement slurry mixing create voids. Although 5% SBL can fill the voids between the fiber-fiber interface and the fiber-cement interface, it is not sufficient to eliminate the aforementioned adverse factors. The pore size distribution of S10E0B0.3 and S10E0B0.6 cement pastes below 100 nm is smaller than that of S5E0B0.6, and the harmful large pore size distribution between 200-1000 nm is smaller than that of S5E0B0.3. This indicates that a 10% SBL mixed with BF can effectively fill the voids caused by the fibers. Figure 8 (b) shows that the cumulative pore size of BF-SBL cement paste decreases with the increase of SBL content. The cumulative pore size of S10E0B0.3 cement paste is smaller than that of the other three groups of cement paste. In summary, with the increase of SBL content, the harmful large pore of cement paste gradually decreases, and the cumulative pore size decreases, which is consistent with the previous analysis.

4. CONCLUSIONS

The main purpose of this study is to investigate the effect of BF-based multi-component systems on oil well cement stone. The fluidity, setting time, density, compressive strength and flexural strength of BF multi-component composite samples were tested. The SEM, XRD, FTIR and MIP were performed on the BF multi-component composite cementitious composites with better performance. The following conclusions can be drawn:

The addition of BF and a small amount of ER into the cement slurry results in the largest decrease in compressive strength of the cement paste, with the 7 days compressive strength at 10.7 MPa, which fails to meet the cementing requirements.

Adding 0.6% BF and 10% SBL into the cement slurry results in good mechanical performance of the cement paste, by effectively controlling the development of microcracks in cement. The 7 d compressive strength and flexural strength are enhanced to 28.6 MPa and 3.7 MPa, respectively.

BF plays a crucial role in bridging and anti-pulling in cement paste, as it controls the width and extension of microcracks. The SBL can effectively fill the gaps between cement particles, fiber-cement matrix interface and fiber-fiber interface, refine the pore size distribution, and thus improve the cement strength.

CONFLICTS OF INTEREST

There are no conflicts of interest to declare.

ACKNOWLEDGEMENTS

This study was financially supported by Sichuan Science and Technology Program (grant number 2023NSFSC0781) and the Everest Scientific Research Program (grant number 80000-2020ZF11411). This study was also supported by Open Fund (grant number PLC20210402) of State Key Laboratory of Oil and Gas Reservoir Geology and Exploitation (Chengdu University of Technology). The authors would like to thank the Shiyanjia Lab (www.shiyanjia.com) for all the teachers who assisted in this experiment.

REFERENCES

B. Zhou, X. Yao, S. D. Hua. The influence of pressure testing of casing string on the integrity of cement sheath, Drilling Fluid & Completion Fluid, 26, (2009), 32-34.

S. M. Zhou, L. Z. Wang, G. Q. Yang, H.Q. Yao. Researches of CO_2 corrosion to cement stone at high temperature, Petroleum Exploration & Production Research Institute, 36, (2008), 9-13.

Y. Liu, H. B. Yan, X. Yu, Y. Q. Feng, W. H. Fan. Negative impacts of borehole pressure change on cement sheath sealing integrity and countermeasures, Natural Gas Industry, 34, (2014), 95-98.

J. Li, M. Chen, H. Zhang, Z. Y. Chen. Influence of cement sheath shape on casing stress under different ground stress conditions, Natural Gas Industry, 24, (2004), 50-52.

Z. Y. Li, X. Y. Guo, F. Q. Luo, Z. X. Dong. Research on mechanism of increasing flexibility and decreasing brittleness of cement sheath in oil well, Acta Petrolei Sinica, 29, (2008), 438-441.

S. D. Hua, X. Yao. Reduction in friability of well cement stone and its function mechanism, Journal of China University of Petroleum (Edition of Natural Science), 31, (2007), 108-112.

M. Li, S. Deng, P. Yan, J. Z. Jin, Y. J. Yu. Research on the toughening mechanism of fiber/whisker on oil well cement stone, Journal of Southwest Petroleum University (Science & Technology Edition), 38, (2016),151-155.

Dhand, V. Mittal, G. Rhee, K.Y. Hui D. A short review on BF reinforced polymer composites, Composites Part B, 73, (2015),166-180.

Y. Li, J. P. Zhang, Y. Z. He, G. J. Huang, J. B. Li, Z. X. Niu, B. Gao. A review on durability of basalt fiber reinforced concrete, Composites Science and Technology, 225, (2022), 109519.

E. Monaldo, F. Nerilli, G. Vairo: Basalt-based fiber-reinforced materials and structural applications in civil engineering, Composite Structures, 214, (2019), 246–263.

X. W. Heng, M. L. Zhang, Y. S. Yang, D. Long, Z. Y. Li, X. Y. Guo: Effects of BF on the performance of aluminate cement stone, Oil Drilling & Production Technology, 38, (2016), 42-47.

H. W. Luo, Z. Y. Li, X. W. Cheng, Y. J. Yi, L. Lin: Study on mechanical performance of low density mineral fiber cement, Drilling Fluid & Completion Fluid, 32, (2015), 76-78.

Z. Gao, P. Cao, X. J. Sun, Y. W. Zhao: Compressive strength analysis and microscopic characterization of BF reinforced concrete, Journal of Hydroelectric Engineering, 37, (2018), 111-120.

B. Qi，J. W. Fu，Q. L. Sun，W. M. Liu，Q. Q. Yu, B. Du，Z. H. Lin, Z. P. Ma: Preparation of styrene-butadiene latex and performance evaluation of oil well cement slurry, Oilfield Chemistry, 33, (2016), 401- 405.

P. Y. Yan, L. Yue, D. Dai, Y. W. Luo: Influence of ER emulsion without curing agent on hydration of oil Well cement in early age, Journal of The Chinese Ceramic Society, 45, (2017), 608-613.

Y. L. Liu, Z. Y. Li, Y. T. Xue, B. Zhou, H. Sun, D. H. Su, J. F. Sun: Study on mechanical properties of cementing waterborne epoxy cement, Bulletin of the Chinese Ceramic Society, 38, (2019), 339-343.

Y. M. Wu, M. b. Xu, J. J. Song, X. l. Wang, J. Zhou: Synergistic effect of carbon fiber and latex on the mechanical properties of cement slurry, Bulletin of the Chinese Ceramic Society, 38, (2019), 253-258.

Z. X. Li, D. H. Liu: Effect of polymer latex and polypropylene fiber on the properties of oil well cement, Contemporary Chemical Industry, 49, (2020), 1437-1440.

M. Y. Zhu, J. S. Qiu, J. X. Chen: Effect and mechanism of coal gangue concrete modification by basalt fiber, Construction and Building Materials, 328, (2022), 126601.

R. Wang, X. G. Li, P. M. Wang: Influence of polymer on cement hydration in SBR-modified cement pastes, Cement Concrete Research, 36, (2006), 1744-1751.

Z. C. Lu, X. M. Kong, Q. Zhang, Y. Cai, Y. R. Zhang, Z. M. Wang, B. Q. Dong, F. Xing: Influences of styrene-acrylate latexes on cement hydration in oil well cement system at different temperatures, Colloids and Surfaces A: Physicochemical and Engineering Aspects, 507, (2016),46–57.

I. Ray, A.P. Gupta, M. Biswas: Effect of latex and superplasticizer on Portland cement mortar in the hardened state, Cement and Concrete Composites, 17, (1995), 9-21.

X. M. Kong, S. Emmerling, J. Pakusch, M. Rueckel, J. Nieberle: Retardation effect of styrene-acrylate copolymer latexes on cement hydration, Cement Concrete Research, 75, (2015),23–41.

M. Shafieyzadeh: Prediction of compressive strength of concretes containing silica fume and styrene-butadiene rubber (SBR) with a mathematical mode, International Journal of Concrete Structures and Materials, 7, (2013), 295-301.

N. Ukrainczyk, A. Rogina: Styrene butadiene latex modified calcium aluminate cement mortar, Cement and Concrete Composites, 41, (2013), 16–23.

C. H. Jiang, K. Fan, F. Wu, D. Chen: Experimental study on the mechanical properties and microstructure of chopped basalt fiber reinforced concrete, Materials & Design, 58, (2014), 187–193.

X. D. Chen, S. X. Wu, J. K. Zhou: Influence of porosity on compressive and tensile strength of cement mortar, Construction and Building Materials, 40, (2013), 869-874.

J. J. Song, M. B. Xu, C. Q. Tan, F. C. You, X. L. Wang, S. S. Zhou: Study on an epoxy resin system used to improve the elasticity of oil well cement-based composites, Materials, 15, (2022), 5258.

Z. Q. Jin, S. C. Li, H. M. Song, Z. Li, D. J. Zhu: Experimental and simulative study of bonding properties on fiber/epoxy interfaces by digital image correlation (DIC) technique and molecular dynamics, Cement and Concrete Composites, 131, (2022), 104569.

S. Khandelwal, K. Y. Rhee, Recent advances in basalt-fiber-reinforced composites: Tailoring the fiber-matrix interface, Composites Part B, 192, (2020), 108011.

F. d. A. Silva, B. Mobasher, R. D. T. Filho: Cracking mechanisms in durable sisal fiber reinforced cement composites, Cement and Concrete Composites, 31, (2009), 721–730.

J. M. L. Reis: Fracture and flexural characterization of natural-fiber-reinforced polymer concrete, Construction and Building Materials, 20, (2006), 673–678.

M, Z, Zhu, B, Chen, M. Wu, J. X. Han: Effects of different mixing ratio parameters on mechanical properties of cost-effective green engineered cementitious composites (ECC), Construction and Building Materials, 328, (2022), 127093.

Y. Y. Yang, Q. Zhou, X. K. Li, G. C. Lum, Y. Deng: Uniaxial compression mechanical property and fracture behavior of hybridinorganic short mineral fibers reinforced cement-based material, Cement and Concrete Composites, 104, (2019), 103338.

D. Li, D. Niu, Q. Fu, D. M. Luo: Fractal characteristics of pore structure of hybrid Basalt–Polypropylene fiber-reinforced concrete, Cement and Concrete Composites, 109, (2020), 103555.

E. Karakosta, L. Lagkaditi, S. ElHardalo, A. Biotaki, V.C. Kelessidis, M. Fardis, G. Papavassiliou: Pore structure evolution and strength development of G-type elastic oilwell cement, A combined HNMR and ultrasonic study, Cement Concrete Research, 72, (2015), 90-97.